



# Deflating the shale gas potential of South Africa's Main Karoo basin

## AUTHORS:

Michiel O. de Kock<sup>1</sup>

Nicolas J. Beukes<sup>1</sup>

Elijah O. Adeniyi<sup>1</sup>

Doug Cole<sup>2</sup>

Annette E. Götz<sup>3</sup>

Claire Geel<sup>4</sup>

Frantz-Gerard Ossa<sup>1</sup>

## AFFILIATIONS:

<sup>1</sup>DST-NRF CIMERA, Department of Geology, University of Johannesburg, Johannesburg, South Africa

<sup>2</sup>Council for Geoscience, Pretoria, South Africa

<sup>3</sup>School of Earth and Environmental Sciences, University of Portsmouth, Portsmouth, United Kingdom

<sup>4</sup>Department of Geological Sciences, University of Cape Town, Cape Town, South Africa

## CORRESPONDENCE TO:

Michiel de Kock

## EMAIL:

mdekock@uj.ac.za

## DATES:

**Received:** 08 Nov. 2016

**Revised:** 10 Mar. 2017

**Accepted:** 10 June 2017

## KEYWORDS:

Ecca Group; Whitehill Formation; hydrocarbon; thermal maturity; energy resource

## HOW TO CITE:

De Kock MO, Beukes NJ, Adeniyi EO, Cole D, Götz AE, Geel C, et al. Deflating the shale gas potential of South Africa's Main Karoo basin. *S Afr J Sci.* 2017;113(9/10), Art. #2016-0331, 12 pages. <http://dx.doi.org/10.17159/sajs.2017/20160331>

## ARTICLE INCLUDES:

- × Supplementary material
- × Data set

## FUNDING:

CIMERA-KARIN

© 2017. The Author(s).  
Published under a Creative Commons Attribution Licence.

The Main Karoo basin has been identified as a potential source of shale gas (i.e. natural gas that can be extracted via the process of hydraulic stimulation or 'fracking'). Current resource estimates of 0.4–11x10<sup>9</sup> m<sup>3</sup> (13–390 Tcf) are speculatively based on carbonaceous shale thickness, area, depth, thermal maturity and, most of all, the total organic carbon content of specifically the Ecca Group's Whitehill Formation with a thickness of more than 30 m. These estimates were made without any measurements on the actual available gas content of the shale. Such measurements were recently conducted on samples from two boreholes and are reported here. These measurements indicate that there is little to no desorbed and residual gas, despite high total organic carbon values. In addition, vitrinite reflectance and illite crystallinity of unweathered shale material reveal the Ecca Group to be metamorphosed and overmature. Organic carbon in the shale is largely unbound to hydrogen, and little hydrocarbon generation potential remains. These findings led to the conclusion that the lowest of the existing resource estimates, namely 0.4x10<sup>9</sup> m<sup>3</sup> (13 Tcf), may be the most realistic. However, such low estimates still represent a large resource with developmental potential for the South African petroleum industry. To be economically viable, the resource would be required to be confined to a small, well-delineated 'sweet spot' area in the vast southern area of the basin. It is acknowledged that the drill cores we investigated fall outside of currently identified sweet spots and these areas should be targets for further scientific drilling projects.

## Significance:

- This is the first report of direct measurements of the actual gas contents of southern Karoo basin shales.
- The findings reveal carbon content of shales to be dominated by overmature organic matter.
- The results demonstrate a much reduced potential shale gas resource presented by the Whitehill Formation.

## Introduction

The potential shale gas resource of the Karoo Supergroup (Figure 1), and specifically the ~30-m thick Whitehill Formation of the Ecca Group, remains highly speculative.<sup>1-7</sup> An original ~18x10<sup>9</sup> m<sup>3</sup> or 485 trillion cubic feet resource estimate<sup>8</sup> – which would make the Karoo basin the fourth largest resource in the world – is certainly grossly inflated. Trillion cubic feet or Tcf is the unit in which widely published resource estimates are quoted and are provided throughout this contribution in brackets wherever resource estimates are listed in SI units. The United States Energy Information Administration downgraded this estimate to place the Karoo basin as the sixth largest global resource at 11x10<sup>9</sup> m<sup>3</sup> (390 Tcf), of which the Whitehill Formation contributed ~6x10<sup>9</sup> m<sup>3</sup> (211 Tcf).<sup>3</sup> Conservative estimates are much smaller. Preliminary scenarios of 0.9–8x10<sup>9</sup> m<sup>3</sup> (32–287 Tcf) were calculated as alternatives to the US estimate.<sup>1</sup> Subsequent work has resulted in best estimates closer to the smaller conservative value cited above. Deterministic gas estimates of 1–1.2x10<sup>9</sup> m<sup>3</sup> (36–42 Tcf) were calculated for the Whitehill Formation.<sup>4</sup> Comparable to this amount is the probabilistic estimate of 1.4x10<sup>9</sup> m<sup>3</sup> (49 Tcf), but with a large uncertainty interval of 0.4–4.9x10<sup>9</sup> m<sup>3</sup> (14–172 Tcf).<sup>5</sup> A speculated technically recoverable shale gas resource of 0.37x10<sup>9</sup> m<sup>3</sup> (13 Tcf) for the Whitehill Formation and 0.54–0.65x10<sup>9</sup> m<sup>3</sup> (19–23 Tcf) recoverable free gas represent the lower end of estimates.<sup>2,6</sup>

The Karoo Supergroup was deposited some 300 to 183 million years ago on the ancient continent Gondwanaland, but is now best represented by a large erosional remnant in southern Africa referred to as the Main Karoo basin (Figure 1).<sup>9,10</sup> Sedimentation in the basin was terminated during Gondwanaland breakup with the emplacement of the Karoo large igneous province (KLIP), which includes an extensive network of dolerite sills and dykes.<sup>11,12</sup> Along the basin's southern margin the Karoo succession attains a maximum composite thickness of 12 km.<sup>10</sup> Here the basin is bound by a narrow zone of deformation known as the Cape Fold Belt (CFB).<sup>13</sup> KLIP intrusions and deformation associated with the CFB distinguishes the Main Karoo basin from other well-known shale gas basins in the world.

Drilling by the Southern Oil Exploration Corporation (SOEKOR) failed to prove the existence of economic conventional hydrocarbon (particularly oil) reservoirs in the southern Main Karoo basin, but with the advent of unconventional gas plays, the basin again received attention.<sup>1-6,8,14</sup> However, current resource estimates may not sufficiently account for thermal degassing and possible gas escape during KLIP emplacement and development of the CFB.<sup>15</sup> Current estimates either include speculative risk factors to account for these effects, or are deterministic for 'sweet spot' areas where these effects are minimised. Quantitatively, however, the actual effect of KLIP intrusions and the CFB is unknown. Within the spatial limits of the current study, both the effects of KLIP intrusions and thermal tectonism of the CFB are illustrated by various maturity indices.

Unfortunately, much of the carbonaceous shales intersected by the SOEKOR cores are deteriorated and unsuitable for evaluating reservoir and source potentials. Recent studies of unweathered shale material have focused on the geothermal history and petro-physical characteristics of shale units at specific points within the basin<sup>6,15-18</sup>, but direct measurements of the actual available gas content of the shale units are lacking.

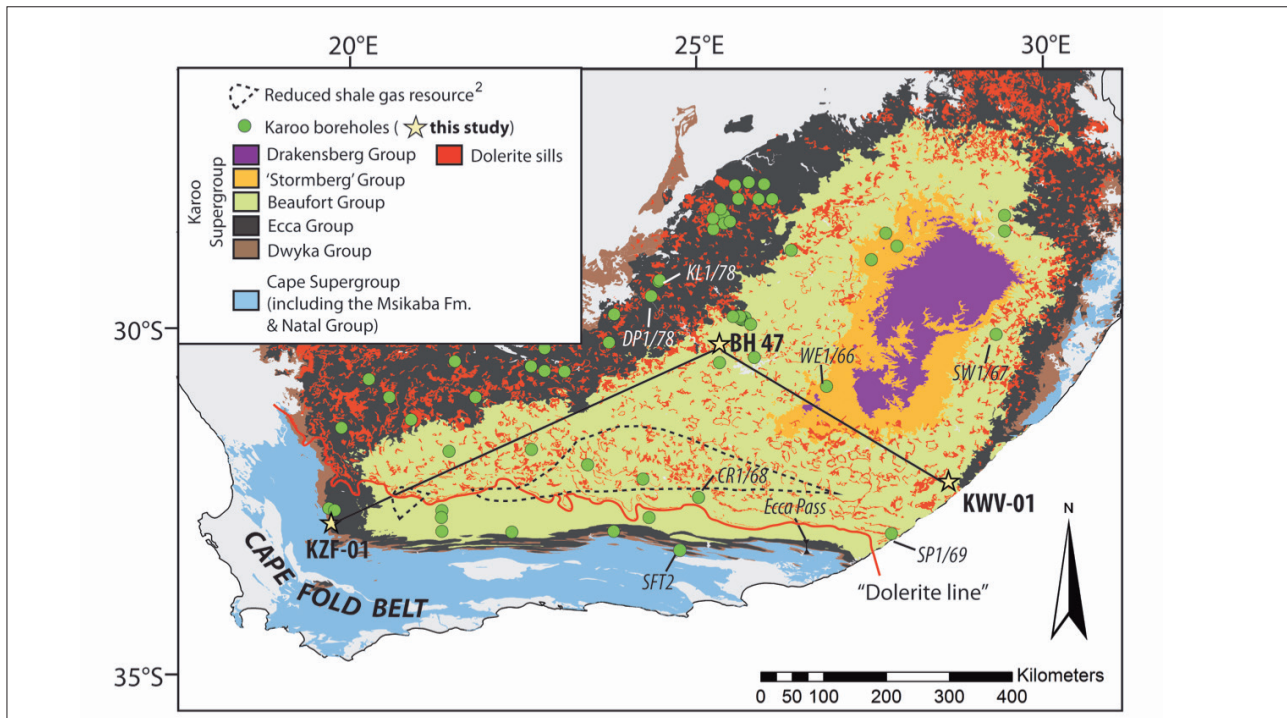


**Figure 1:** Simplified geological map of the Main Karoo basin showing the location of the three drill cores studied and other sites mentioned in the text.

The Karoo Research Initiative (KARIN) under the DST-NRF Centre of Excellence for Integrated Mineral and Energy Resource Analysis (CIMERA) hosted by the University of Johannesburg and co-hosted by the University of the Witwatersrand drilled two boreholes to assist in this endeavour (Figure 1; KZF-01 in the Tankwa Karoo and KVV-01 near Willowvale in the Eastern Cape Province). A borehole drilled by Gold Fields Ltd near Philippolis in the Free State Province to explore the basement rocks of the Karoo succession provides an intersection from the central part of the basin (Figure 1; BH 47).

## Geological setting

Borehole KZF-01 intersects 657 m of the Eccca Group in the southwestern part of the basin near the CFB, but south of the so-called 'dolerite line' — a boundary south of which no dolerite sills are present (Figures 1 and 2). The Whitehill Formation, with a thickness of 19.5 m, was intersected at 420.46 m below the surface, but unexpected structural duplication by low-angle thrust faults or brittle deformation features resulted in further intersections between 443.30 m and 479.55 m (36 m thickness) and between 489.15 m and 498.45 m (9 m thickness). It is difficult to determine the true thickness of the Whitehill Formation given the brecciated nature of contacts, but the first 19.5 m intersection is likely to represent the true thickness as it appears that it is the Prince Albert Formation, rather than the Collingham Formation, that is tectonically displaced with the Whitehill Formation (Figure 2). The shale reservoir is too shallow to be of commercial interest as the depth of shale should be more than 1500 m for safe hydraulic fracturing. Although there is an increased risk of gas escape at depths of less than 1000 m, it should be noted that even at shallow depth any residual gas will remain in place, as will desorbed and free gas, if a suitable caprock is in place. In proximity to the CFB, the Collingham Formation overlying the Whitehill Formation has been shown to have the properties of a suitable caprock as a result of the large proportion of clay minerals, a low total organic carbon content (TOC), the fine-grained nature of lithologies, a low porosity, a lack of permeability, a moderate fracturability, average density values, and the laminate nature of the formation.<sup>17</sup> Near the surface (<200 m) at Loeriesfontein, in the southwestern part of the basin, gas has been escaping from the Whitehill Formation for the past 30 years after a dolerite sill above the formation was breached by a borehole.<sup>19</sup> In the northern part of the basin, near Evander, conventional free gas was

discovered in sandstone of the Vryheid Formation at depths of less than 200 m, and only escaped because of extensive drilling.<sup>20</sup> There is thus very little reason to believe that borehole KZF-01 would not give a realistic reflection of the available gas in the region, despite the Whitehill Formation being at a depth of 420.46 m.

Borehole KVV-01 was drilled in an area known to contain abundant dolerite sills, but little information was available on the nature of the stratigraphic succession. The nearest reference sections are more than 100 km away, represented by SOEKOR cores SP1/69, WE1/66, and SW1/67, and outcrops along the Eccca Pass near Grahamstown (Figure 1).<sup>21</sup> The borehole was drilled to a depth of 2353 m commencing within the Beaufort Group, intersecting the entire Eccca Group and ending within the Dwyka Group (Figure 2). The Whitehill Formation, with its ubiquitous black carbonaceous shale, is dramatically thinner (13 m) than the average of ~39 m in other parts of the southern Karoo basin<sup>2</sup>, and is intruded by a 19-m-thick dolerite sill (Figure 2). The low thickness of the Whitehill Formation in borehole KVV-01 renders it commercially unviable as a shale gas reservoir, and complements a predicted pinch-out of the formation some 65 km to the northeast near Coffee Bay. What was unexpected is the thick sand-dominated Ripon Formation representing much of the Eccca Group with a well-developed interstratified dark grey shale known as the Wonderfontein Member (Figure 2).

The third borehole (BH 47) from which samples were investigated intersected the Eccca and Dwyka groups down into the basement. Thick dolerite sills are characteristic features. The Whitehill Formation could not positively be identified because it is in an area immediately north of the pinch-out. However, samples near the base of the Eccca Group and above the Dwyka Group appear highly carbonaceous and thus this unit is tentatively suggested as being a lateral facies equivalent of the Whitehill Formation (Figure 2). This core is important because it (1) contains several thick dolerite sills and (2) is distal to the effects of the CFB.

Although both new KARIN boreholes were located near the present day erosional margins of the Main Karoo basin, it is important to realise that the Whitehill Formation cannot necessarily be seen as being proximal. In fact, palynofacies analyses indicate marine conditions during the deposition of the Whitehill black shales in the southern Karoo basin.

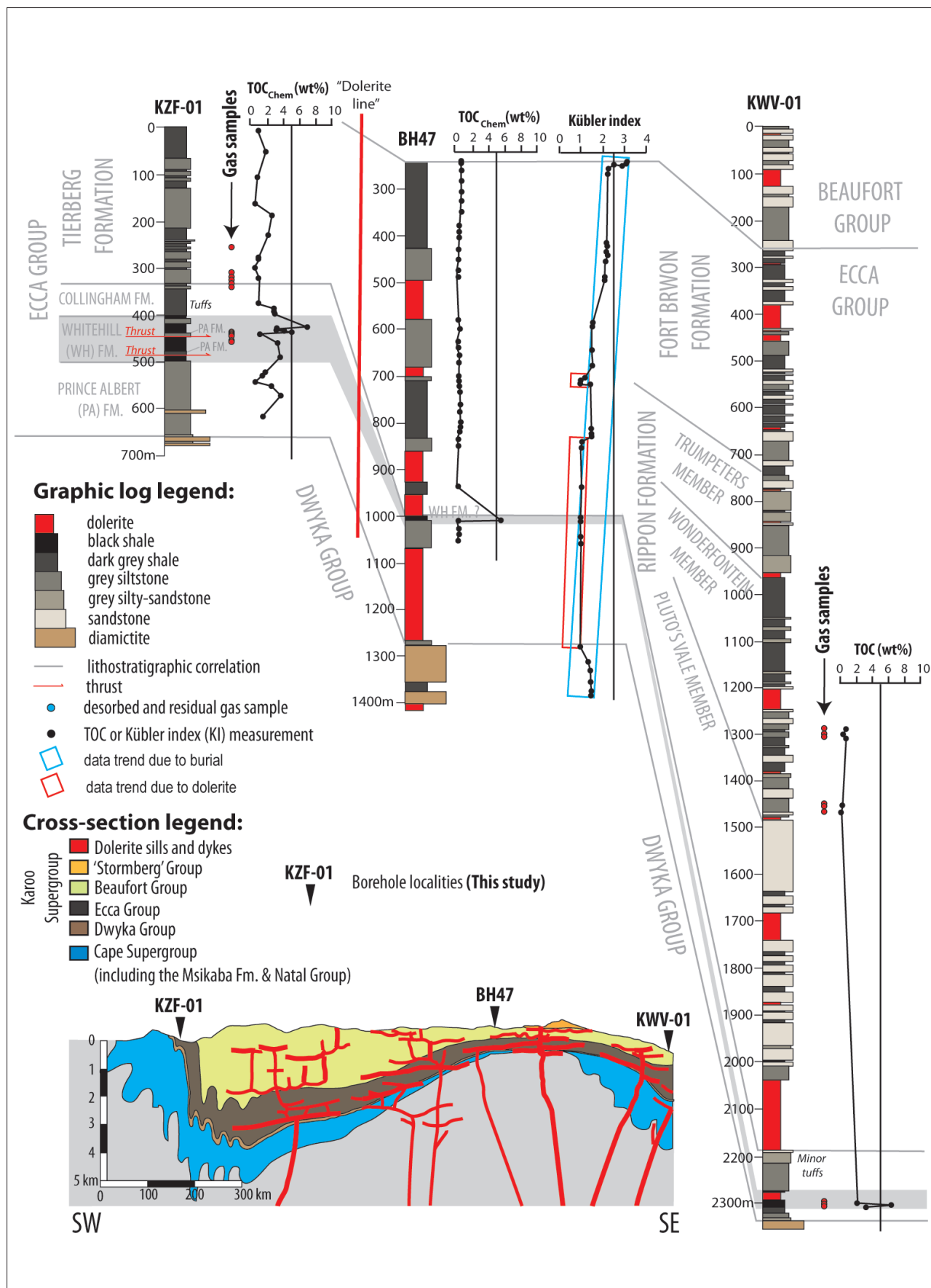


**Figure 2:** Simplified lithostratigraphic logs of boreholes KZF-01, BH 47 and KVV-01 showing the stratigraphic distribution of desorbed and residual gas samples, total organic carbon (TOC<sub>chem</sub>) content, and Kübler index values. Also shown is a schematic cross section (SW-SE) of the southern Karoo basin between the three cores studied.

In the southwestern part of the basin (KZF-01), palynofacies data point to a distal basinal setting with moderate marine phytoplankton percentages (i.e. acritarchs and prasinophytes), good amorphous organic matter preservation, low terrestrial input, and low spores:bisaccates ratios.<sup>22</sup> In the southeastern part of the basin (KVV-01), palynofacies analysis suggests a stratified deep basin setting with low marine phytoplankton percentages (i.e. prasinophytes), good amorphous organic matter preservation, high terrestrial input, and moderate spores:bisaccates ratios.<sup>22</sup> In contrast, a marginal marine, restricted setting was detected in the northern part of the basin (SOEKOR borehole DP 1/78) as documented by low marine phytoplankton percentages (i.e. leiospheres and prasinophytes), low amorphous organic matter preservation, high terrestrial input, and moderate spores:bisaccates ratios.<sup>22</sup>

## Methods

In both boreholes KZF-01 and KVV-01, carbon-rich shale of the Whitehill Formation, together with a few other carbonaceous shale beds in the Eccla Group, were monitored for desorbed gas volume at the drill sites, and later analysed for desorbed gas composition and residual gas volume and composition (Figure 2). Organic carbon was characterised by measurements of TOC content and Rock-Eval pyrolysis. In borehole BH 47, the Prince Albert, Whitehill and Collingham formations could not be distinguished (Figure 2). Here, the Eccla Group is dominated by dark blue-grey shale. TOC content and Rock-Eval pyrolysis values were determined for shale samples in all three cores using the Kübler index, and vitrinite reflectance analyses were performed on samples from core BH 47 near Phillipolis.

### Desorbed and residual gas content and composition

Gas is generated during the maturation of organic matter in shale, and the majority of this gas is typically sorbed or attached to the surface of clay and mud particles. Upon a reduction in pressure, such as that experienced during drilling, some of the gas will desorb, which can be monitored over time at the drill site. We sampled prominent black carbonaceous shale units intersected for desorbed gas measurements on site. There were no apparent gas kicks or blow-outs detected at either of the drilling sites at any stage. Any remaining gas is residual, and it is only released during complete fracturing of the host shale by milling in a vacuum-sealed vesicle. Desorbed and residual gas content and composition of carbonaceous shales in KZF-01 and KVV-01 were monitored by Geokrak (Poland) and by Latona Consulting (South Africa).

For desorption analyses of KZF-01, 20 core samples each of about 300 mm in length were selected from carbonaceous units and transferred

to leak-tight stainless steel canisters in a Geokrak field laboratory immediately after sampling (Figure 3a). The time elapsed between starting a drill run, core retrieval, and eventual sample selection was carefully monitored to account for any lost gas. Accounting for lost gas can have a large effect, but in this case it did not alter the results significantly. Air was removed from the canisters by displacement with helium from a pressurised cylinder. The canisters were closed tight with an expansive plug, weighed and placed in a thermostatic heater. The desorbed gas volume, released as samples were allowed to equilibrate to ambient temperatures in a thermostatic heater, was measured with a volumeter at set time intervals. Initially the readings were made at regular, short intervals. As the gas volume diminished, the interval between readings was lengthened. Desorption of cores was terminated when a single reading of gas volume measured in a 24-h cycle was smaller than 5 cm<sup>3</sup>, or if the amount of desorbed gas released by a core sample in 7 days was less than 1% of the total gas desorbed from the sample. The amount of gas released from core samples was expressed in volume unit per mass unit.

Desorption analyses of KVV-01 was comparably accomplished by Latona Consulting at the drill site. They used leak-tight PVC canisters without displacement of air with helium and without the use of a thermostatic heater. Lost gas, or gas released before samples were sealed, was calculated graphically. Plotting the cumulative desorbed gas in millilitres against the square root of time produced a straight line for about 10 h after coring, and the straight line was projected backwards before the time when the canister was sealed to estimate the lost gas.

One sample of desorbed gas was selected on site from KVV-01 via a plastic pipette for analysis of its content by gas chromatography at the South African Nuclear Energy Corporation (NECSA) in Pretoria, South Africa.

For the residual gas measurements, pieces from each core sample (KZF-01 and KVV-01) were collected when desorption was finished, and milled in a leak-tight stainless steel vessel (Figure 3b) at the respective laboratories of Geokrak and Latona Consulting in Poland and Johannesburg. Measurements of residual gas were made with a volumeter after specified time intervals of milling. The standard milling time was extended from 60 min to 120 min if no gas was released.

Pipettes of residual gas from KZF-01 were collected during residual gas analyses and were subsequently analysed for contents by gas chromatography at NECSA in Pretoria, South Africa, and at the Oil and Gas Institute in Cracow, Poland.

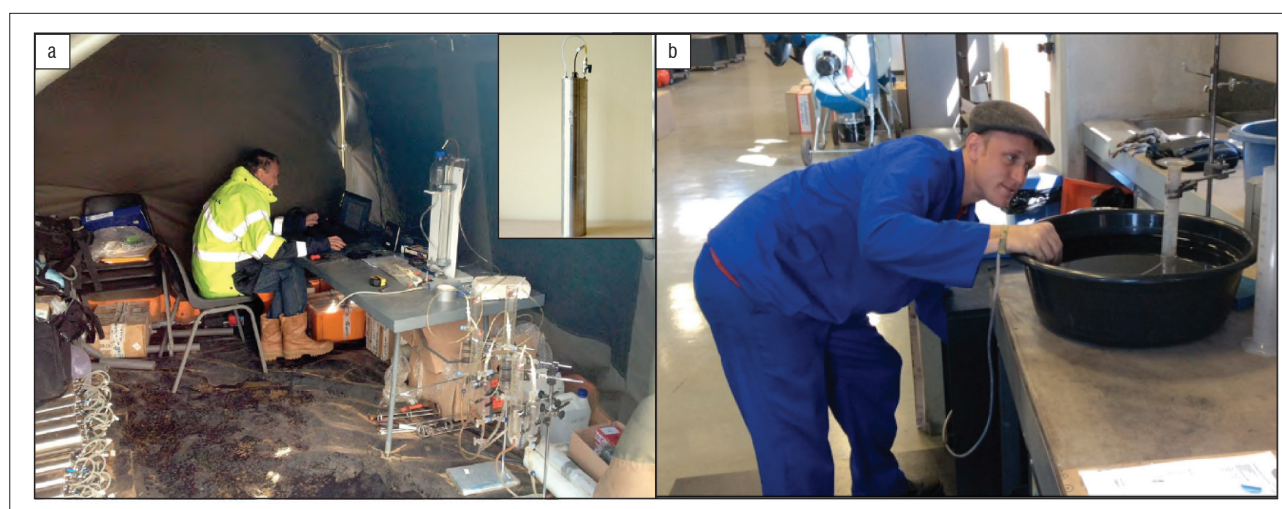


**Figure 3:** (a) Geokrak's desorption field laboratory at the KZF-01 drill site. The inset shows a leak-tight stainless steel desorption canister. (b) Measurement of residual gas content of a milled shale sample at Latona Consulting's Johannesburg laboratory.

### Total organic carbon content 'chemical' method

For the total organic carbon content 'chemical' method ( $\text{TOC}_{\text{chem}}$ ), carbonaceous shale samples were selected from cores of boreholes BH 47 (38 samples) and KZF-01 (26 samples). Samples were cut and milled and 5 g of rock powder per sample was selected for analysis. Samples from BH 47 were analysed at the Institute for Geology and Palaeontology of the University of Münster in Germany. The samples from KZF-01 were analysed at the Department of Geology, University of Maryland in the USA. The TOC content was determined via sealed tube combustion.<sup>23</sup> Between 10 mg and 500 mg of rock powder was decarbonated in a quartz tube with HCl (25%), washed to neutrality and dried at 40 °C. Subsequently, ca 1.5 g of CuO was added and the quartz tubes were sealed under vacuum. CO<sub>2</sub> was liberated from the sample powder via combustion at 850 °C for 3 h, cryogenically purified, quantified and packed in a 6-mm break-seal tube. Analytical performance was monitored using several international (USGS 24, IAEA 40) and in-house laboratory (coal) standards.

### Vitrinite reflectance

Seven samples were selected from BH 47 of carbonaceous shale units both proximal and distal to the dolerite intrusions. Samples were prepared according to the ASTM D7708–14 standard test method for microscopic determination of the reflectance of vitrinite dispersed in sedimentary rocks.<sup>24</sup> Whole-rock samples were mounted in 30-mm moulds with epoxy resin and allowed to cure overnight. Individual mounts were polished to produce a smooth plane surface using a Struers Tegramin polisher. The random reflectance measurement procedures<sup>24</sup> were followed using a Zeiss Axio Imager M2, retrofitted with a Hilgers Fossil Diskus system. Both petrographic identification and vitrinite reflectance readings were determined under non-polarised light. Mean random vitrinite reflectance ( $R_v\text{Vmr}$ ) was measured in percentages of the intensity of reflected light illuminated on a polished plane surface of the rock sample covered with immersion oil by a calibrated microscope or photometer with an x50 oil objective. An average of 32 to 98 vitrinite measurements were taken per sample, depending on the availability of organic matter, and the mean values were determined.

### Kübler index

The Kübler index (KI)<sup>25</sup> was determined using X-ray diffraction analysis at the University of Johannesburg's SPECTRUM. X-ray diffraction analyses were performed using the Panalytical X'Pert Pro X-ray diffractometer with an X'Celerator detector, the CuK $\alpha$  radiation operated at 40 kV and 40 mA. KI was determined for oriented clay particles (<2  $\mu\text{m}$ ) separated from six samples. Air-dried oriented clay separates (<2  $\mu\text{m}$  particles) were prepared by placing mildly crushed sample material in lidded bottles that were half-filled with osmosis water before being placed in an ultrasonic bath for over 3 h for separating clay particles from the detrital minerals (e.g. quartz and feldspars). The bottles were placed in a fume box for a minimum of 8 h to allow the solutions to attain room temperature or ~20 °C. The solution was then shaken and left for 2.5 h to allow a suspension of <2  $\mu\text{m}$  particles from the solution according to Stoke's Law.<sup>26</sup> The water with suspended clay particles was pipetted into a clean beaker and placed in an oven at 40 °C to dry out the water and collect the fine clay-rich powders.

KI was also determined from 37 bulk rock samples. KI is calculated as the width at half-height of an illite peak at 10 Å. Results obtained from clay-rich separates are consistent with those from bulk rock analysis. Therefore, KI values of bulk rocks were used to complete the KI trend across the borehole.

### Rock-Eval pyrolysis

Shale samples were evaluated using a Rock-Eval 6 pyrolyser at the Department of Earth Sciences of the Indian Institute of Technology, India. Powdered sample material was pyrolysed in an inert atmosphere and the residual carbon was subsequently burnt in an oxidation oven. The amount of hydrocarbons released ( $S_1$  and  $S_2$ ) during the pyrolysis between 300 °C and 650 °C, later increased to 750 °C at a rate of 25 °C/min, were detected with a flame ionisation detector. Free hydrocarbons

are designated as  $S_1$  and hydrocarbons generated with further thermal cracking are designated as  $S_2$ . The temperature at which hydrocarbon yield is maximised is termed  $T_{\text{max}}$ . The gases released during the pyrolysis [CO and CO<sub>2</sub> ( $S_3$ )] were detected with an online infrared detector continuously throughout the process.<sup>27</sup> Any remaining carbon after pyrolysis is residual ( $S_4$ ). The TOC content from pyrolysis ( $\text{TOC}_{\text{pyro}}$ ) is not directly measured, but can be calculated as a weight percentage using Equation 1:

$$\text{TOC}_{\text{pyro}} = [0.082(S_1 + S_2) + S_4]/10, \quad \text{Equation 1}$$

where 0.082 is a constant representing the average amount of carbon from thermally extracted and pyrolysed hydrocarbons.<sup>28</sup>

Several indices can be calculated to evaluate the geochemistry of the organic matter as well as its thermal maturity.<sup>27</sup> The hydrogen index or HI, determined by Equation 2, provides a measure of the relative amount of organic matter still capable of producing petroleum, sometimes referred to as 'live' organic matter. The production index or PI is calculated using Equation 3 and provides an estimate of the extent to which oil generation has taken place. The oxygen index or OI is defined by Equation 4 and provides a measure of the amount of organic bound oxygen in the sample.

$$\text{HI} = S_2/\text{TOC}_{\text{pyro}} \times 100 \quad \text{Equation 2}$$

$$\text{PI} = S_1/(S_1 + S_2) \quad \text{Equation 3}$$

$$\text{OI} = S_3/\text{TOC}_{\text{pyro}} \times 100 \quad \text{Equation 4}$$

## Results

Desorbed gas contents of samples were very low (Table 1). The largest volume (0.22 m<sup>3</sup>/t) was obtained from the Wonderfontein Member in KVV-01, but was only a small initial desorbed volume. Desorbed gas was essentially carbon dioxide with very little methane at a concentration of 4.8 ppm. Samples yielded little or, as was the case for KVV-01, no residual gas. KZF-01 yielded inconsistent residual gas volumes (0.00–0.74 m<sup>3</sup>/t; Table 1). The Whitehill Formation did not contain elevated gas content. Residual gas was mostly methane (61–99%), with variable concentrations of nitrogen and carbon dioxide (Table 2).

$\text{TOC}_{\text{chem}}$  of samples ranges between 0.01 wt% and 6.83 wt% (Figure 2; Table 3). Content is generally low for shale samples of the Tierberg (0.44–2.54 wt%) and Collingham formations (0.91–2.87 wt%) in KZF-01 (Table 3) and higher for the Whitehill Formation (1.19–6.83 wt%). The Prince Albert Formation has a very variable, but overall low  $\text{TOC}_{\text{chem}}$  (0.47–3.64 wt%).  $\text{TOC}_{\text{chem}}$  is very low in BH 47 (0.04–0.42 wt%), but one sample considered correlative with the Whitehill Formation at a depth of 1011.25 m yielded 5.59 wt%. This concentration is comparable to that of the Whitehill and Prince Albert formations in KZF-01. The Whitehill Formation's average  $\text{TOC}_{\text{chem}}$  content in our boreholes (i.e. 3.77 wt% in KZF-01 based on eight samples and 5.59 wt% in one sample from BH 47) is generally above the 2 wt% qualifying value employed in original shale gas resource estimation, but lower than the 6 wt% average on which resource estimates were based.<sup>1,8</sup>

Vitrinite reflectance measurements (Figure 4) of BH 47 Eccla Group shale samples that lie further away from dolerite sills display unexpectedly higher values (3.71–3.91%), compared to those closer to dolerite sills (1.17–1.77%). Organic matter fragments are rare and generally very small. Samples far away from dolerite intrusions appear to have no structure or orientation, have very fine-grained and shattered organic matter amongst coarser quartz grains and framboidal pyrite (Figure 5a and 5b), while samples closer to intrusions have an apparent orientation of organic matter, which is layered and networked around quartz particles with pyrite inclusions (Figure 5c and 5d). The organic matter is generally highly matured and appears as solid bitumen networks, and is more likely to be inertinite than vitrinite. Reflectance values are thus better referred to as total reflectance rather than vitrinite reflectance.

**Table 1:** Gas content of KZF-01 and KVV-01 core samples

Borehole	Formation or Member	Sample number	Core interval (in m)		Desorbed gas	Residual gas	Total gas
			from	to			
KZF-01	Tierberg	BIZ-84/01/D	262.08	262.38	0.01	0.12	0.13
		BIZ-84/02/D	312.26	312.56	0.01	n.a.	n.a
		BIZ-84/03/D	319.38	319.77	0.01	n.a.	n.a
		BIZ-84/04/D	323.05	323.45	0.01	0.41	0.45
		BIZ-84/05/D	329.10	329.40	0.01	n.a.	n.a
	Collingham	BIZ-84/06/D	340.83	341.13	0.00	0.27	0.27
	Whitehill	BIZ-84/07/D	422.10	422.34	0.00	0.11	0.11
		BIZ-84/08/D	423.32	423.62	0.00	0.24	0.24
		BIZ-84/09/D	425.10	425.40	0.00	0.18	0.18
		BIZ-84/10/D	426.24	426.56	0.00	n.a.	n.a
		BIZ-84/11/D	428.10	428.38	0.00	n.a.	n.a
		BIZ-84/12/D	429.10	429.40	0.00	n.a.	n.a
		BIZ-84/13/D	431.10	431.39	0.01	0.22	0.23
		BIZ-84/14/D	432.29	432.57	0.00	0.17	0.17
		BIZ-84/15/D	434.04	434.34	0.01	n.a.	n.a.
		BIZ-84/16/D	435.55	435.85	0.00	n.a.	n.a.
		BIZ-84/17/D	437.08	437.38	0.00	0.00	0.00
		BIZ-84/18/D	438.54	438.82	0.01	n.a.	n.a.
		BIZ-84/19/D	447.80	448.17	0.01	0.74	0.75
		BIZ-84/20/D	449.35	449.64	0.00	0.56	0.56
KVV-01		Wonderfontein	LT01	1291.27	1292.27	0.20	0.00
	LT02		1303.27	1304.27	0.00	0.00	0.00
	LT03		1309.27	1310.27	0.03	0.00	0.03
	Pluto's Vale	LT04	1450.27	1451.27	0.02	0.00	0.02
		LT05	1453.27	1454.27	0.01	0.00	0.01
		LT06	1465.27	1466.27	0.05	0.00	0.05
	Whitehill	LT07	2295.02	2295.52	0.01	0.00	0.01
		LT08	2299.39	2299.59	0.00	0.00	0.00
		LT09	2305.39	2305.89	0.00	0.00	0.00

n.a., not analysed

**Table 2:** Residual gas composition in KZF-01

Formation	Sample number	Air free gas components (%)		
		CH <sub>4</sub>	N <sub>2</sub>	CO <sub>2</sub>
Tierberg	BIZ-84/04/D	99.10	0.00	0.90
Collingham	BIZ-84/06/D	99.72	0.00	0.28
Whitehill	BIZ-84/08/D/R	68.89	7.59	22.70
	BIZ-84/13/D	61.38	38.46	0.15
	BIZ-84/14/D/R	68.78	7.90	22.17
	BIZ-84/19/D	83.91	0.00	26.09
	BIZ-84/20/D/R	85.83	3.45	10.24

**Table 3:** Total organic carbon (TOC<sub>chem</sub>) content of shale samples

Borehole	Formation	Sample number <sup>†</sup>	TOC <sub>chem</sub> (in wt%)
KZF-01	Tierberg	KZF-14.36	0.85
		KZF-55.74	1.77
		KZF-113.79	0.72
		KZF-164.41	0.44
		KZF-189.38	2.54
		KZF-231.7	2.08
		KZF-275.95	0.96
		KZF-279.81	1.12
		KZF-299.1	0.36
		KZF-323.59	1.01
	Collingham	KZF-376.82	0.91
		KZF-385.58	2.78
		KZF-398.10	2.87
	Whitehill	KZF-424.5	6.83
		KZF-428.79	3.38
		KZF-431.36	3.17
		KZF-431.65	3.79
		KZF-434.34	5.02
		KZF-438.82	1.19
		KZF-458.1	3.23
KZF-488.1		3.55	
Prince Albert	KZF-518.1	1.93	
	KZF-540.43	0.47	
	KZF-549.08	2.47	
	KZF-568.63	3.64	
	KZF-611.76	1.34	
BH 47	Undifferentiated	BH47-242.80	0.35
		BH47-244.50	0.33
		BH47-247.40	0.37
		BH47-261.37	0.39
		BH47-283.15	0.39
		BH47-308.15	0.42
		BH47-328.00	0.37
		BH47-350.82	0.32
		BH47-381.97	0.20
		BH47-392.40	0.19
		BH47-408.50	0.15
		BH47-434.50	0.07
		BH47-455.50	0.08
		BH47-478.50	0.05
		BH47-495.00	0.05
		BH47-586.00	0.07
		BH47-605.00	0.23
		BH47-632.00	0.06
		BH47-644.27	0.05
		BH47-660.60	0.19
		BH47-678.00	0.14
		BH47-706.00	0.07
		BH47-716.09	0.13
		BH47-726.02	0.18
		BH47-741.12	0.24
		BH47-766.64	0.28
		BH47-782.56	0.26
		BH47-804.51	0.31
		BH47-814.82	0.25
	BH47-824.83	0.25	
	BH47-842.00	0.05	
	BH47-854.30	0.08	
	BH47-939.00	0.04	
Whitehill?	BH47-1011.25	5.59	
Undifferentiated	BH47-1018.00	0.06	
	BH47-1033.00	0.09	
	BH47-1047.00	0.13	
	BH47-1060.50	0.05	

<sup>†</sup>Sample numbers correspond to depth in metres

Published vitrinite reflectance data from the Main Karoo basin are limited, but suggest general increasing maturity ( $R_o = 1.0\%$  to  $4.3\%$ ) for the Whitehill Formation from the north to the south of the basin for samples unaffected by dolerite sills – a trend that reflects the tectonic front of the CFB.<sup>6,14,29</sup> Samples affected by dolerite sills exhibit a higher reflectance of up to  $8.8\%$ .<sup>29</sup> The total reflectance values obtained here for Eccca Group shales from BH 47 fit the expectation, but the very low total reflectance values from Eccca Group shale in proximity to dolerite sills is unexpected. The fine-grained nature of organic matter and lack of clearly identifiable vitrinite in samples close to dolerites place a caution on these measurements.

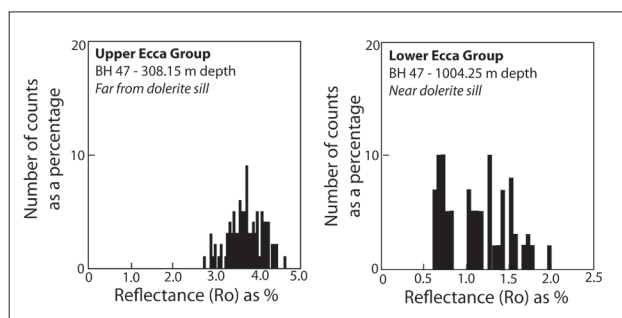
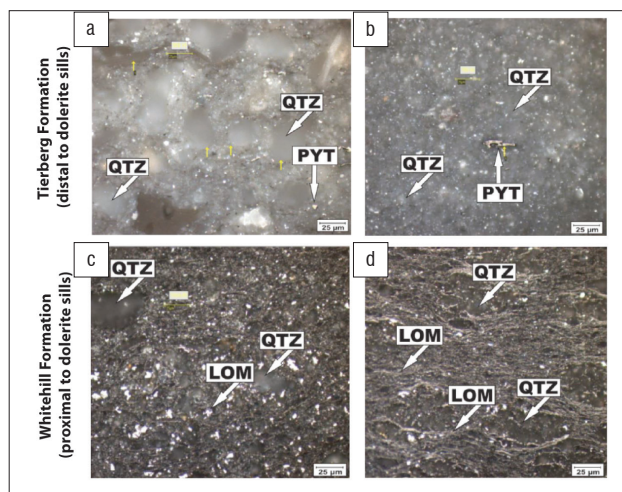


**Figure 4:** Examples of vitrinite reflectance data plotted as histograms for carbonaceous shale samples from borehole BH 47 distal from dolerite sills and in proximity to dolerite sills.



QTZ, quartz; PYT, pyrite; LOM, layered organic matter.

**Figure 5:** Petrographic images of carbonaceous shale samples from BH 47. (a) Upper Eccca Group shale (Tierberg Formation?) at 308.15 m depth distal from dolerite sills. (b) Upper Eccca Group shale (Tierberg Formation?) at 766.64 m depth distal from dolerite sills. (c) Whitehill Formation equivalent at 1004.63 m depth in proximity to a dolerite sill. (d) Whitehill Formation equivalent at 1011.25 m depth in proximity to a dolerite sill.

A progressive decrease of the KI values represents a gradual increase in non-expandable illite layers and the disappearance of the expandable smectite layers in the smectite-illite mixed layers as depth increases.<sup>30</sup> Within the Main Karoo basin, KI values reveal a north–south increasing effect of burial maturity and range from  $>5$  in the north to  $>3$  in the south for shales from outcrops.<sup>14,18</sup> In BH 47, KI values range from 3.15 near the surface to 1.50 at a depth of 1385 m (Figure 2; Table 4). Most of the samples yield values below 2.50, which marks the onset of metamorphic conditions (Figure 2). In addition, a local trend is seen with KI dropping to as low as 1.00 as contacts with dolerite sills are approached (Figure 2).

**Table 4:** Kübler index of shale samples from BH 47 with relative stratigraphic position of dolerite sills indicated

Borehole	Formation	Sample number <sup>†</sup>	Kübler index	
BH 47	Undifferentiated	BH47-242.80	3.15	
		BH47-244.50	3.10	
		BH47-247.40	2.54	
		BH47-251.70	2.36	
		BH47-255.86	2.30	
		BH47-267.26	2.25	
		BH47-416.58	2.20	
		BH47-422.01	2.20	
		BH47-434.50	2.18	
		BH47-455.50	2.15	
		BH47-489.00	2.10	
		BH47-495.00	2.10	
		Dolerite sill		
		BH47-586.00	1.58	
		BH47-595.00	1.55	
	BH47-644.27	1.53		
	BH47-678.00	1.51		
	Dolerite sill			
	BH47-706.00	1.20		
	BH47-711.59	1.00		
	BH47-715.00	1.00		
	BH47-716.09	1.00		
	BH47-718.99	1.40		
	BH47-819.32	1.47		
	BH47-824.83	1.50		
	BH47-830.00	1.50		
	BH47-842.00	1.09		
	BH47-854.30	1.05		
	Dolerite sill			
	BH47-932.00	1.05		
	Dolerite sill			
	Whitehill?	BH47-1004.6	1.01	
	BH47-1011.25	1.01		
Undifferentiated	BH47-1047.00	1.00		
	BH47-1060.50	1.00		
	Dolerite sill			
	BH47-1280.70	1.00		
	BH47-1313.11	1.30		
	BH47-1333.00	1.35		
	BH47-1357.84	1.40		
	BH47-1377.94	1.48		
BH47-1385.12	1.50			

<sup>†</sup>Sample numbers correspond to depth in metres

Pyrograms obtained during Rock-Eval pyrolysis analyses of carbonaceous shale samples reveal low amounts of free hydrocarbon ( $S_1$ ) and poorly defined  $S_2$  (hydrocarbons released by thermal cracking) peaks (Figure 6), which results in unreliable constraints of  $T_{max}$  and low thermal maturity indices such as the hydrogen and production indices (Table 5). The hydrocarbon generation potential of the organic matter or kerogen is generally poor (calculated as the sum of  $S_1$  and  $S_2$ ; Figure 7a) despite promising  $TOC_{Pyro}$  contents calculated from pyrolysis. The low hydrogen index suggests that much of the organic matter is not bound to hydrogen, and that hydrocarbon generation could have taken place in the past. Much of the organic carbon is thus 'dead' carbon. If hydrocarbon generation occurred in the basin, then it was not readily preserved as suggested by

the low production index and the low volumes of residual gas. Organic matter or kerogen is of poor quality in terms of hydrocarbon generating potential according to a scheme that compares the production index with  $TOC_{Pyro}$ .<sup>31</sup> Poor quality kerogen is also seen elsewhere in the basin (Figure 7a).<sup>6,29,32</sup> Generally, kerogen is either gas-prone Type III kerogen or Type IV kerogen (Figure 7b). The former is the likely final residue of a pre-existing kerogen type that has completely matured (i.e. 'dead' organic carbon). However, kerogen in borehole DP1/78 near Hopetown in the northern part of the basin (Figure 1) displays a thermal evolution trend of a Type I kerogen (oil prone), the maturation trend of which is now within the wet and dry gas domain (Figure 7).<sup>33</sup> This finding further supports the overmature nature of pre-existing kerogen.

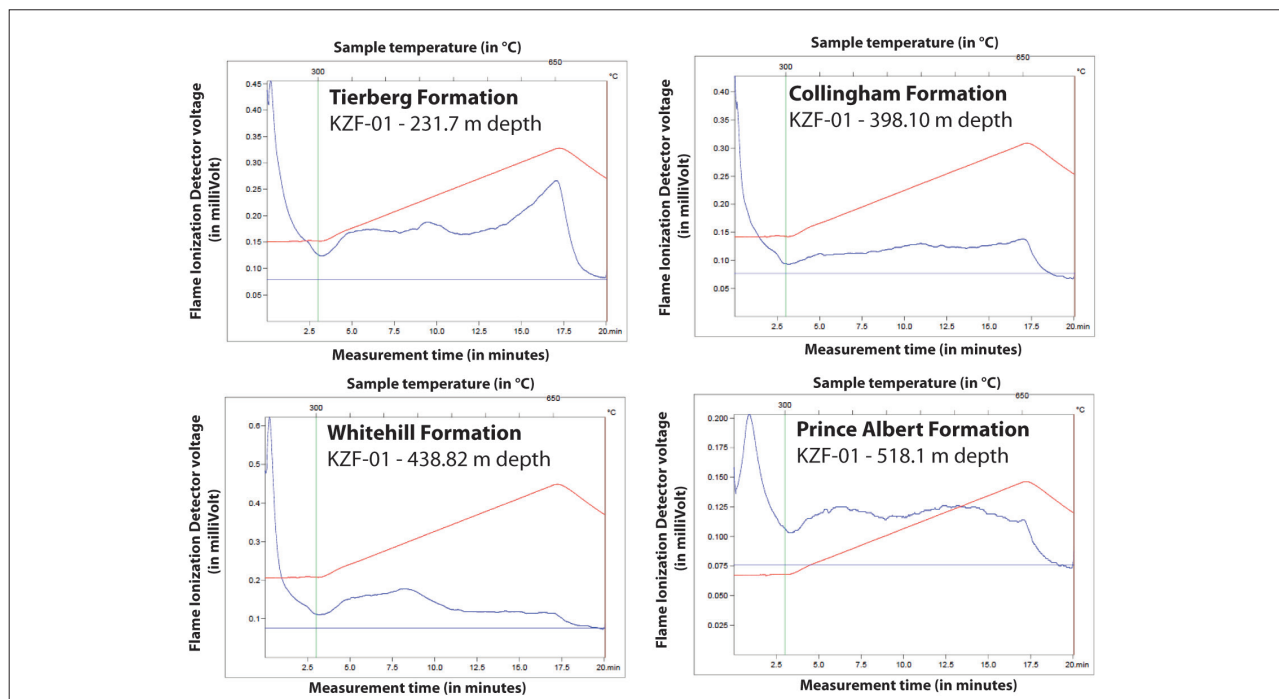


Figure 6: Selected pyrograms obtained of carbonaceous shale samples from KZF-01.

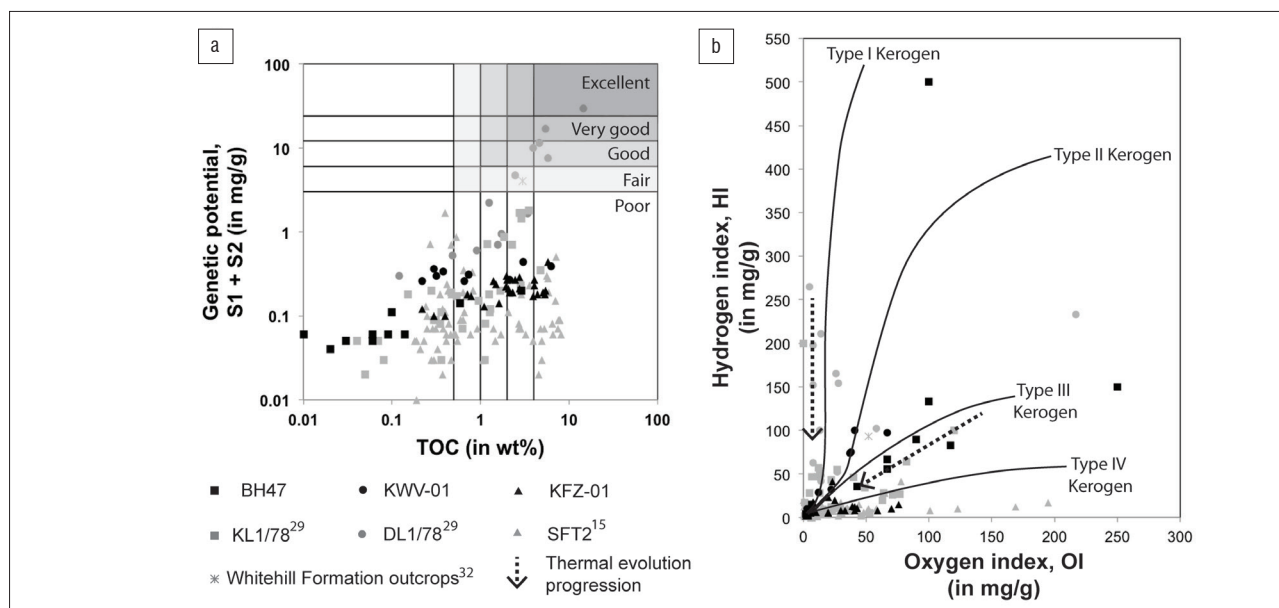


Figure 7: (a) Classification of kerogen quality in the Ecca Group carbonaceous shales.<sup>31</sup> (b) A modified Krevelen diagram<sup>31</sup> indicates the dominance of Type III and IV kerogen in Ecca Group shales of KZF-01, BH 47 and KVV-01 with reference to other studies in the Karoo basin as indicated.

**Table 5:** Summary of Rock-Eval pyrolysis results

Borehole	Formation or Member	Sample number <sup>†</sup>	S <sub>1</sub>	S <sub>2</sub>	T <sub>max</sub>	S <sub>3</sub>	TOC <sub>Pyro</sub> <sup>‡</sup>	HI	OI	PI	
			(mg/g)		(°C)	(mg/g)	(wt%)				
KZF-01	Tierberg	KZF-14.36	0.06	0.18	604	0.61	1.5	12	41	0.25	
		KZF-55.74	0.08	0.18	603	0.55	1.41	13	39	0.31	
		KZF-113.79	0.05	0.12	607	0.59	0.78	15	76	0.29	
		KZF-164.41	0.08	0.22	604	0.84	1.97	11	43	0.27	
		KZF-189.38	0.08	0.19	605	1.38	1.98	10	70	0.30	
		KZF-231.7	0.06	0.23	604	1.13	2.77	8	41	0.21	
		KZF-275.95	0.05	0.16	605	0.62	2.07	8	30	0.24	
		KZF-279.81	0.05	0.14	606	0.45	2.3	6	20	0.26	
		KZF-299.1	0.07	0.14	605	0.56	2.77	5	20	0.33	
	Collingham	KZF-323.59	0.08	0.19	605	0.8	2.45	8	33	0.30	
		KZF-376.82	0.05	0.14	605	0.12	2.13	7	6	0.26	
		KZF-385.58	0.04	0.1	604	0.16	1.63	6	10	0.29	
	Whitehill	KZF-398.10	0.04	0.09	602	0.65	1.1	8	59	0.31	
		KZF-424.5	0.08	0.12	388	0.2	5.46	2	4	0.40	
		KZF-428.79	0.08	0.1	322	0.17	4.37	2	4	0.44	
		KZF-431.36	0.05	0.13	396	0.1	5.33	2	2	0.28	
		KZF-431.65	0.06	0.21	607	0.25	4.06	5	6	0.22	
		KZF-434.34	0.06	0.17	392	0.17	4.06	4	4	0.26	
		KZF-438.82	0.07	0.12	382	0.1	5.11	2	2	0.37	
		KZF-458.1	0.04	0.13	605	0.14	3.92	3	4	0.24	
	Prince Albert	KZF-488.1	0.08	0.36	392	0.23	5.76	6	4	0.18	
		KZF-518.1	0.03	0.09	488	0.05	0.22	41	23	0.25	
		KZF-540.43	0.02	0.08	491	0.1	0.4	20	25	0.20	
		KZF-549.08	0.03	0.07	503	0.06	0.3	23	20	0.30	
		KZF-568.63	0.05	0.13	344	0.06	0.71	18	8	0.28	
	BH 47	Undifferentiated	KZF-611.76	0.06	0.16	304	0.09	1.93	8	5	0.27
			BH47-369.51	0.02	0.09	416	0.09	0.1	90	90	0.18
			BH47-416.58	0.01	0.05	492	0.07	0.06	83	117	0.17
BH47-711.59			0.01	0.03	336	0.05	0.02	150	250	0.25	
BH47-756.64			0.01	0.05	493	0.06	0.09	56	67	0.17	
BH47-790.25			0.01	0.05	584	0.06	0.14	36	43	0.17	
Whitehill?		BH47-819.32	0.01	0.04	494	0.04	0.06	67	67	0.20	
		BH47-1011.25	0.08	0.12	300	0.07	2.87	4	2	0.40	
Undifferentiated		BH47-1274.80	0.01	0.05	491	0.01	0.01	500	100	0.17	
		BH47-1360.44	0.01	0.04	492	0.03	0.03	133	100	0.20	
	BH47-1377.94	0.05	0.09	449	0.04	0.59	15	7	0.36		
KVV-01	Wonderfontein	KVV-1291.27	0.07	0.19	481	0.08	0.66	29	12	0.27	
		KVV-1303.27	0.06	0.28	441	0.14	0.38	74	37	0.18	
		KVV-1309.27	0.07	0.24	498	0.16	0.74	32	22	0.23	
	Pluto's Vale	KVV-1450.27	0.06	0.24	427	0.12	0.32	75	38	0.20	
		KVV-1453.27	0.07	0.29	473	0.2	0.3	97	67	0.19	
		KVV-1465.27	0.04	0.22	437	0.09	0.22	100	41	0.15	
	Whitehill	KVV-2295.02	0.06	0.21	338	0.07	2.12	10	3	0.22	
		KVV-2299.39	0.12	0.27	429	0.23	6.27	4	4	0.31	
KVV-2305.39	0.16	0.28	299	0.22	3.04	9	7	0.36			

<sup>†</sup>Sample numbers correspond to depth in metres. <sup>‡</sup>TOC<sub>Pyro</sub> determined during Rock-Eval pyrolysis.

## Discussion

Our data indicate that heating by dolerite sills in boreholes KVV-01 and BH 47 and burial metamorphism in boreholes KZF-01 and BH 47 have resulted in the elevated thermal maturity of organic matter and the destruction of hydrocarbon potential in our samples. Negligible amounts of desorbed and residual gas volumes suggest that natural gas, if generated sometime in the geological history of the strata (rock succession), was not preserved in KZF-01 and KVV-01. Although gas generation probably did occur, much gas was likely lost via thermal degassing at KVV-01 and tectonic deformation (possibly through thrusting with increased load) at KZF-01. Contact metamorphism by dolerite sills has resulted in catastrophic and explosive degassing and alteration of shale, but no textural evidence was encountered in the boreholes of this study.<sup>34</sup> A high thermal gradient can lead to overmaturity of organic matter and the production of bitumen derived from hydrocarbons, which can migrate and solidify in fractures.<sup>35</sup> Although such vein-like deposits were not encountered in our boreholes, it was noted that organic matter in the black shale at 1011.25 m in BH 47 appears as solid bitumen networks of inertinite.

The reservoir potential of high maturity shales is not well understood, but for the Marcellus Shale of the Appalachian basin in North America it has been suggested that regional metamorphism may have destroyed the shale reservoir's porosity and self-sealing capacity.<sup>36</sup> A high thermal gradient related to burial, tectonism or increased mantle heat flow may have overmatured the organic matter in the Karoo shales, such that the porosity and self-sealing capacity of the Whitehill Formation was destroyed leading to the non-preservation of gas. Gas was not preserved as shale gas in any of our boreholes. It is possible that gas was generated, but this gas likely escaped to be trapped locally in rare instances. Such trapped conventional gas was most probably encountered in SOEKOR borehole CR 1/68 (Figure 1)<sup>14</sup>, where gas was found hosted in fractured shale of the Fort Brown Formation. This gas could have escaped from the underlying Whitehill Formation. Very small gas and oil shows have been recorded from the less mature northern part of the Main Karoo basin.<sup>14,20</sup> However, high-volume gas shows like that of CR 1/68 have not been encountered often, suggesting that it is a rare occurrence.

It is unclear at this stage if there remain significant areas of conventional and unconventional gas retention by shale in the basin. Such areas are likely low-risk 'sweet spots'<sup>2,4,5</sup>, and are expected to have lower thermal maturity, to be relatively free of dolerite intrusions, and to have additional suitable attributes (e.g. in respect of burial depth and thickness). It should be noted that CR 1/68 is located just south of such a sweet spot defined by low-risk segment mapping (i.e. low or no dolerite volume in the Whitehill Formation).<sup>2,5</sup> The apparent rare occurrence of higher volume gas shows is thus perhaps a function of the small number of boreholes that intersect such low-risk sweet spots. The most recent attempts to estimate the shale gas resource of the Karoo basin have endeavoured to identify such sweet spots by interpolating sparse legacy data.<sup>2,4,6</sup> These areas represent the most realistic shale gas resource in the Main Karoo basin, but their real gas potential remains to be tested. Furthermore, the confident identification of such areas ultimately requires an as yet unreached level of understanding of dolerite sill distribution and dynamics throughout the basin. Such understanding is subject to the acquisition of high-resolution geophysical data.

Another significant outcome of the KARIN research is that TOC values are variable and generally lower than the average values used during original shale gas resource estimations.<sup>1,8</sup> The distal setting of the Whitehill Formation in KZF-01 and KVV-01 would suggest that the determined TOC values are representative. With an average TOC content of 3.77 wt%, the Whitehill Formation in KZF-01 (arguably the most distal of all our samples) is significantly lower than the 6 wt% average used in original estimations, but perhaps more comparable to the 4.55 wt% estimate for sweet spots.<sup>2</sup> Much more important are Rock-Eval analyses results that indicate most of the organic matter to be fully burned or 'dead' carbon, with little hydrocarbon-generating potential remaining. The carbonaceous shales at some stage after their deposition likely yielded large volumes of hydrocarbons but very little of that appears to have been preserved at the sites investigated, other than the occurrence of sparse, fracture-filled, vein-like deposits of pseudocoal, which represent solidification of viscous bitumen derived from hydrocarbons.<sup>35</sup>

## Conclusion

Regional heterogeneity in organic carbon content and thermal maturity, although accounted to some extent in shale gas resource estimates of the southern Main Karoo basin, may pose a greater risk towards low hydrocarbon generation and preservation. Our results indicate that carbon content is very variable, even within the same formation at a specific locality within the basin. The original resource estimates are thus likely highly inflated, although even much lower estimates are of commercial interest, given that, for example, the Mosgas project was initiated on an initial resource (reserve base) of  $0.03 \times 10^9 \text{ m}^3$  (1.0 Tcf).<sup>37</sup> We show that hydrocarbon generation and preservation is negatively affected by an elevated thermal gradient and dolerite intrusions. In addition to the localised effect of dolerite intrusions, we identify the significant risk posed by an increased thermal gradient (as a result of burial, tectonism or increased mantle heat flow) towards shale gas generation and preservation. A high thermal gradient likely resulted in overmaturity of organic matter in the Whitehill Formation and destruction of its porosity and self-sealing capability. Quantification of the real resource should be limited to 'thermal oases', in which shale gas was generated and preserved. Such areas are expected to have low or no dolerite volume in the Whitehill Formation. Very likely the most realistic resource estimates for the Karoo basin are between  $0.37 \times 10^9 \text{ m}^3$  and  $1.4 \times 10^9 \text{ m}^3$  (13–49 Tcf), with the lower estimate perhaps being the most realistic given the sparsity of data.<sup>2,4,6</sup> This estimation is supported by our study, in which samples distal from dolerite sills in BH 47, situated in an area far away from the CFB, are also overmature. Thus, it is expected that rocks in so-called sweet spots near Beaufort West and Sutherland (but closer to the CFB) should show the same, or even higher, maturity.

A comparison of data from the Whitehill Formation with that of the shale gas producing Barnett Shale in Texas indicates a gas resource of about  $0.37 \times 10^9 \text{ m}^3$  (13 Tcf) in areas where the Whitehill Formation is at depths of more than 1500 m, contains less than 20% dolerite, and has a vitrinite reflectance of <3.5% (Figure 1).<sup>2</sup> Proving this resource is crucial, and a very important next step is testing it within an identified sweet spot, as is currently planned by the Council for Geoscience through drilling of an additional scientific stratigraphic borehole near Beaufort West.<sup>38</sup>

## Acknowledgements

We acknowledge support from CIMERA which administered the KARIN funding, made possible through a donation by Shell. We thank the communities of the Tankwa Karoo and Willowvale for their support and ongoing interest. We thank Geoserve Exploration Drilling and Alec Birch for management of the drilling programme. We acknowledge the support staff of CIMERA (i.e. Ms Viwe Koti and Mr George Henry) for their contribution towards the execution of the project.

## Authors' contributions

Project management and leadership was shared by M.O.d.K. and A.E.G., with significant contributions by N.J.B. A.E.G. was responsible for initial funding acquisition. M.O.d.K. wrote the initial draft, with all authors contributing during advanced stages of writing. E.O.A. is a master's student under supervision of M.O.d.K. and co-supervision of N.J.B. and F.G.O. Detailed lithostratigraphic logs of the CIMERA-KARIN cores were made by D.C. Borehole BH 47 was sampled by M.O.d.K., while sampling of the KZF-01 and KVV-01 was conducted by the KARIN researchers, including N.J.B., A.E.G., M.O.d.K., D.C. and C.G. Kübler index data were collected by E.O.A. and F.G.O., and vitrinite reflectance measurements were made by E.O.A. C.G. provided Rock-Eval data from elsewhere in the basin for comparison purposes.

## References

1. Decker J, Marot J. Annexures: Investigation of hydraulic fracturing in the Karoo of South Africa. Pretoria: Department of Mineral Resources; 2012. Available from: <http://www.dmr.gov.za/publications/viewdownload/182/854.html>.
2. Cole D. Geology of Karoo shale gas and how this can influence economic gas recovery. Gas – The game changer for South Africa?! Paper presented at: Fossil Fuel Foundation Conference; 2014 May 12; Johannesburg, South Africa.

3. Kuuskraa V, Stevens S, Van Leeuwen T, Moodhe K. World shale gas and shale oil resource assessment. Technically recoverable shale oil and shale gas resources: An assessment of 137 shale formations in 41 countries outside the United States. Washington DC: US Department of Energy; 2013. Available from: <http://www.eia.gov/analysis/studies/worldshalegas/pdf/fullreport.pdf>.
4. Mowzer Z, Adams S. Shale gas prospectivity analysis of the southern Main Karoo basin. Petroleum Agency South Africa contribution to the strategic environmental assessment. Agency report FG 2015. Cape Town: Petroleum Agency South Africa; 2015.
5. Decker J. Geological evaluation of the Karoo basin's shale gas resource. Paper presented at: 4th Shale Gas Southern Africa Summit; 2014 March 24–26; Cape Town, South Africa.
6. Geel C, De Wit MJ, Booth PWK, Schulz H-M, Horsfield B. Palaeo-environment, diagenesis and characteristics of Permian black shales in the lower Karoo Supergroup flanking the Cape Fold Belt near Jansenville, Eastern Cape, South Africa: Implications for the shale gas potential of the Karoo basin. *S Afr J Geol*. 2015;118(3):249–274. <http://dx.doi.org/10.2113/gssajg.118.3.249>
7. Cole DI, Basson WA. Whitehill Formation. In: Johnson MR, editor. South African Committee for Stratigraphy Lithostratigraphic Series 3. Preoria: The Council for Geoscience; 1991. p. 51–53.
8. Kuuskraa V, Stevens S, Van Leeuwen T, Moodhe K. World shale gas resources: An initial assessment of 14 regions outside the United States. Washington DC: United States Energy Information Administration; 2011. Available from: <http://www.eia.doe.gov/analysis/studies/worldshalegas>.
9. Catuneanu O, Wopfner H, Eriksson PG, Cairncross B, Rubidge BS, Smith RMH, et al. The Karoo basins of south-central Africa. *J Afr Earth Sci*. 2005;43(1–3):211–253. <http://dx.doi.org/10.1016/j.jafrearsci.2005.07.007>
10. Johnson MR, Van Vuuren CJ, Hegenberger WF, Key R, Shoko U. Stratigraphy of the Karoo Supergroup in southern Africa: An overview. *J Afr Earth Sci*. 1996;23(1):3–15. [http://dx.doi.org/10.1016/S0899-5362\(96\)00048-6](http://dx.doi.org/10.1016/S0899-5362(96)00048-6)
11. Jourdan F, Féraud G, Bertrand H, Kampunzu AB, Tshoso G, Watkeys MK, et al. Karoo large igneous province: Brevity, origin, and relation to mass extinction questioned by new <sup>40</sup>Ar/<sup>39</sup>Ar age data. *Geology*. 2005;33(9):745. <http://dx.doi.org/10.1130/g21632.1>
12. Svensen H, Corfu F, Polteau S, Hammer Ø, Planke S. Rapid magma emplacement in the Karoo Large Igneous Province. *Earth Planet Sci Lett*. 2012;325–326:1–9. <http://dx.doi.org/10.1016/j.epsl.2012.01.015>
13. Hansma J, Tohver E, Schrank C, Jourdan F, Adams D. The timing of the Cape Orogeny: New <sup>40</sup>Ar/<sup>39</sup>Ar age constraints on deformation and cooling of the Cape Fold Belt, South Africa. *Gondwana Res*. 2016;32:122–137. <http://dx.doi.org/10.1016/j.gr.2015.02.005>
14. Rowsell DM, De Swardt AMJ. Diagenesis in Cape and Karoo sediments, South Africa, and its bearing on their hydrocarbon potential. *Trans Geol Soc S Afr*. 1976;79:81–145.
15. Geel C, Schulz H-M, Booth P, De Wit M, Horsfield B. Shale gas characteristics of Permian black shales in South Africa: Results from recent drilling in the Ecca Group (Eastern Cape). *Energy Procedia*. 2013;40:256–265. <http://dx.doi.org/10.1016/j.egypro.2013.08.030>
16. Maré LP, De Kock MO, Cairncross B, Mouri H. Application of magnetic geothermometers in sedimentary basins: An example from the Western Karoo basin, South Africa. *S Afr J Geol*. 2014;117(1):1–14. <http://dx.doi.org/10.2113/gssajg.117.1.1>
17. Black DE, Booth PWK, De Wit MJ. Petrographic, geochemical and petro-physical analysis of the Collingham Formation near Jansenville, Eastern Cape, South Africa – Potential cap rocks to shale gas in the Karoo. *S Afr J Geol*. 2016;119(1):171–186. <http://dx.doi.org/10.2113/gssajg.119.1.171>
18. Smithard T, Bordy EM, Reid DL. The effect of dolerite intrusions on the hydrocarbon potential of the lower Permian Whitehill Formation (Karoo Supergroup) in South Africa and southern Namibia: A preliminary study. *S Afr J Geol*. 2015;118(4):489–510. <http://dx.doi.org/10.2113/gssajg.118.4.489>
19. Macey PH, Siegfried HP, Minaar H, Almond J, Botha PMW. The geology of Loeriesfontein area. Explanation: Sheet 3018. Pretoria: Council for Geoscience; 2011.
20. Van Vuuren CJ, Broad DS, Jungslager EHA, Roux J, McLachlan IR. Oil and gas. In: Wilson MGC, Anhaeusser C, editors. The mineral resources of South Africa. Pretoria: Council for Geoscience; 1998. p. 483–494.
21. Kingsley CS. Stratigraphy and sedimentology of the Ecca Group in the Eastern Cape Province, South Africa [PhD thesis]. Port Elizabeth: University of Port Elizabeth; 1977.
22. Götz AE, Ruckwied K. Palynology of the Permian Prince Albert and Whitehill Formations (Karoo basin, South Africa): New insights on basin dynamics and implications for shale gas exploration. Paper presented at: Joint meeting of TSOP-AASP-ICCP; 2016 Sep 18–23; Houston, Texas, USA.
23. Strauss H, Des Marais DJ, Hayes JM, Lambert IB, Summons RE. Procedures of whole rock and kerogen analysis. In: Schopf JW, Klein C, editors. The Proterozoic biosphere: A multidisciplinary study. Cambridge: Cambridge University Press; 1992. p. 699–707. <https://doi.org/10.1017/CBO9780511601064.018>
24. ASTM International. Standard test method for microscopical determination of reflectance of vitrinite dispersed in sedimentary rocks (D7708-14). West Conshohocken, PA: ASTM International; 2016 [cited 2017 Feb 15]. Available from: <http://www.astm.org>
25. Kübler B. Les argiles indicateurs de métamorphisme [The clay mineral indicators of metamorphism]. *Revue Institut de la Français de Pétrole*. 1964;19:1093–1112. French.
26. Batchelor GK. An introduction to fluid dynamics. Cambridge: Cambridge University Press; 1967.
27. Lafargue E, Marquis F, Pillot D. Rock-Eval 6 applications in hydrocarbon exploration, production, and soil contamination studies. *Revue de l'Institut Français du Pétrole*. 1998;53(4):421–437. <https://doi.org/10.2516/ogst:1998036>
28. Espitalie J, Marquis F, Barsony I. Geochemical logging, Project B70 81018 Geology No. 25457. Paris: Institut Francais du Pétrole; 1982.
29. Aarnes I, Svensen H, Polteau S, Planke S. Contact metamorphic devolatilization of shales in the Karoo basin, South Africa, and the effects of multiple sill intrusions. *Chem Geol*. 2011;281:181–194. <http://dx.doi.org/10.1016/j.chemgeo.2010.12.007>
30. Eberl DD, Velde B. Beyond the Kübler index. *Clay Miner*. 1989;24:571–577.
31. Dembicki H. Three common source rock evaluation errors made by geologists during prospect or play appraisals. *Am Assoc Pet Geol Bull*. 2009;93:341–356. <http://dx.doi.org/10.1306/10230808076>
32. Summons RE, Hope JM, Swart R, Walter MR. Origin of Nama basin bitumen seeps: Petroleum derived from a Permian lacustrine source rock traversing southwestern Gondwana. *Org Geochem*. 2008;39:589–607. <http://dx.doi.org/10.1016/j.orggeochem.2007.12.002>
33. Cole DI, McLachlan IR. Oil potential of the Permian Whitehill Shale Formation in the Main Karoo basin, South Africa. In: Ulbrich H, Rocha Campos AC, editors. Gondwana Seven Proceedings; 1988 July 18–22; Sao Paulo, Brazil. Sao Paulo: Instituto de Geociências, Universidade de Sao Paulo; 1991. p. 379–390.
34. Svensen H, Jamtvit B, Planke S, Chevallier L. Structure and evolution of hydrothermal vent complexes in the Karoo basin, South Africa. *J Geol Soc London*. 2006;163:671–682. <https://doi.org/10.1144/1144-764905-037>
35. Cole DI, Roberts DL. Other carbonaceous fuels. In: Wilson MGC, Anhaeusser C, editors. The mineral resources of South Africa. Pretoria: Council for Geoscience; 1998. p. 495–504.
36. Laughrey CD, Ruble TE, Lemmens H, Kostelnik J, Butcher AR, Walker G, et al. Black shale diagenesis: Insights from integrated high-definition analyses of post-mature Marcellus Formation rocks, Northern Pennsylvania. Paper presented at: American Association of Petroleum Geologists Annual Convention and Exhibition; 2011 April 10–13; Houston, Texas, USA.
37. Van der Spuy D. An overview of South Africa's oil and gas landscape. Proceedings of the 2nd SAMREF Meeting; 2016 October 27; Cape Town, South Africa. Cape Town: South African Marine Research and Exploration Forum; 2016.
38. Malumbazo N, Chevalier L. CGS stratigraphic borehole. *Geobulletin*. 2016;59(1):30–34.

